# Classification of Tissue Oxygenation Properties based on Simultaneous Dynamic $\Delta R_1$ and $\Delta R_2$* D(C)$O_2$E-MRI

**S. Remmele[1], A. Müller[2], F. Träber[2], I. Wenningmann[3], M. von Lehe[4], J. Gieseke[2,5], S. Flacke[2,6], W. A. Willinek[2], H. H. Schild[2], J. Keupp[1], and P. Mürtz[2]**
[1]Philips Research Laboratories, Hamburg, Germany, [2]Department of Radiology, University of Bonn, Bonn, Germany, [3]Department of Anesthesiology, University of Bonn, Bonn, Germany, [4]Department of Neurosurgery, University of Bonn, Bonn, Germany, [5]Philips Healthcare, Best, Netherlands, [6]Department of Radiology, Lahey Clinic, Tufts University Medical School, MA, United States

## Introduction

The monitoring of respiratory challenges with dynamic (C)$O_2$-enhanced (D(C)$O_2$E) MRI is gaining increasing interest for the assessment of tumor oxygenation, vasoreactivity, vessel maturity and function, all being important parameters that decide about optimal treatment strategies [1,2]. The two major research directions propagate either the measurement of $R_1$ or $R_2$* during (C)$O_2$ breathing to monitor the voxel concentrations of the two endogenous "contrast agents" altered by arterial $pO_2$, blood flow and volume changes: dissolved molecular $O_2$ ($mO_2$) and the deoxygenated hemoglobin fraction (dHb). Being paramagnetic agents, both increase $R_1$ and $R_2$* with $R_1$ primarily representing $mO_2$ [3] and $R_2$* primarily representing dHb [4], respectively. Consequently, preclinical studies have recently shown [5,6] that the investigation of both effects increases the specificity of D(C)$O_2$E MRI. These studies either performed simultaneous $R_1$ and $R_2$* weighted imaging or quantified $R_1$ and $R_2$* in sequential and separate measurements. To avoid additional experiments and thus to improve accuracy and time efficiency in clinical applications, we devised an approach to simultaneous and dynamic $\Delta R_1$, $\Delta R_2$* quantification and applied it to patients and a volunteer. The multi-parametric findings are related to tissue-specific properties of intracranial tumors.

## Methods

Informed consent was obtained from 4 patients with intracranial tumors (metastasis, 2 glioblastoma, lymphoma) and a volunteer. All underwent a respiratory challenge with 1/4/2min of air/carbogen/air breathing [7]. Dynamic and simultaneous $R_1$ and $R_2$* quantification is based on a spoiled gradient-echo short-TR sequence with multiple echoes as described in [8] with a temporal resolution of 2.2s/frame: $R_2$* is obtained from the multi-echo signal decay, $R_1$ is obtained from the steady-state signal $M_0$ and an a-priori $R_{1,0}$ and $B_{1,0}$ measurement. Dynamic protocol: 2D, TR=98ms, 12 echoes, $\alpha$=25°, 1.8x1.8x5mm$^3$, REST slabs above and below the imaging slice. $R_{1,0}$ [9]: MS, TSE-factor = 40, 1.8x1.8x5mm$^3$, $TR_{IR}/TR_{SE}$=3s/1.3s, $B1_0$: AFI, 3D, $\alpha$=50°, $TR_{1,2}$= 19ms, 79ms, 3.6x3.6x3mm$^3$. Imaging was carried out on a 3T clinical scanner (Philips Achieva TX, The Netherlands) using a solenoid head coil. From the dynamic $\Delta R_1$ and $\Delta R_2$* series, $\Delta R_1$ and $\Delta R_2$* response maps were generated that depict the voxel-wise amplitude of the response to an (C)$O_2$ challenge as described in [10] after motion-correction and registration of all a-priori and dynamic data. Edema, necrotic, and enhancing tumor regions, as confirmed by standard MRI, were segmented as well as gray and white matter and CSF based on the $R_{1,0}$ map. The tissue-specific voxel-wise response amplitudes in the segmented areas were plotted in $\Delta R_1$ over $\Delta R_2$* plots. The processing workflow is outlined in **Fig. 1**.

## Results and Discussion

The $\Delta R_1$, $\Delta R_2$* response of gray and white matter ("normal vascularization") clustered in the left upper quarter of the $\Delta R_1$, $\Delta R_2$* plot, which is consistent with a decrease in dHb and an increase in $mO_2$ during carbogen breathing. Necrotic tissue, edema, and CSF (high liquid content) were located in the right upper quarter, which is consistent with a dominant $mO_2$ effect. The response in enhancing tumor area of the lymphoma did not differ from that in grey and white matter, whereas for the glioblastomas and the metastasis (**Fig. 2**) a relevant amount of voxels with large negative $\Delta R_2$* values were found. In combination with the high baseline $R_2$* value in that area (not shown), this suggests a high blood volume with a low baseline oxygen saturation ($SO_2$) and thus a dominant impact of the dHb decrease on $R_2$* and $R_1$. Our findings suggest that, based on the $R_1$ and $R_2$* response to elevated $O_2$ levels, tissue can be classified according to its dHb and $mO_2$ properties, respectively (**Fig. 3**). E.g. Areas of low blood volume and well vascularized areas with high baseline $SO_2$ cannot be distinguished by $\Delta R_2$* alone (both show low $\Delta R_2$*) but they differ in $\Delta R_1$.On the other hand, in areas with low baseline $SO_2$, $R_2$* will decrease with the decreasing dHb content, whereas the $R_1$ response might be less pronounced due to the dominant dHb effect that counteracts any $mO_2$ related $R_1$ increase [4].

## Conclusion

Previous studies of dynamic $R_2$* or $R_1$ changes in response to oxygen-enriched air inhalation gave insight into blood and tissue oxygenation properties, although the interpretation becomes difficult in the absence of a significant $R_2$* or $R_1$ response. Simultaneous dynamic $R_1$ and $R_2$* measurements provide information on both, the effects of dHb and $mO_2$, and are therefore expected to increase the specificity of (C)$O_2$-enhanced MRI.

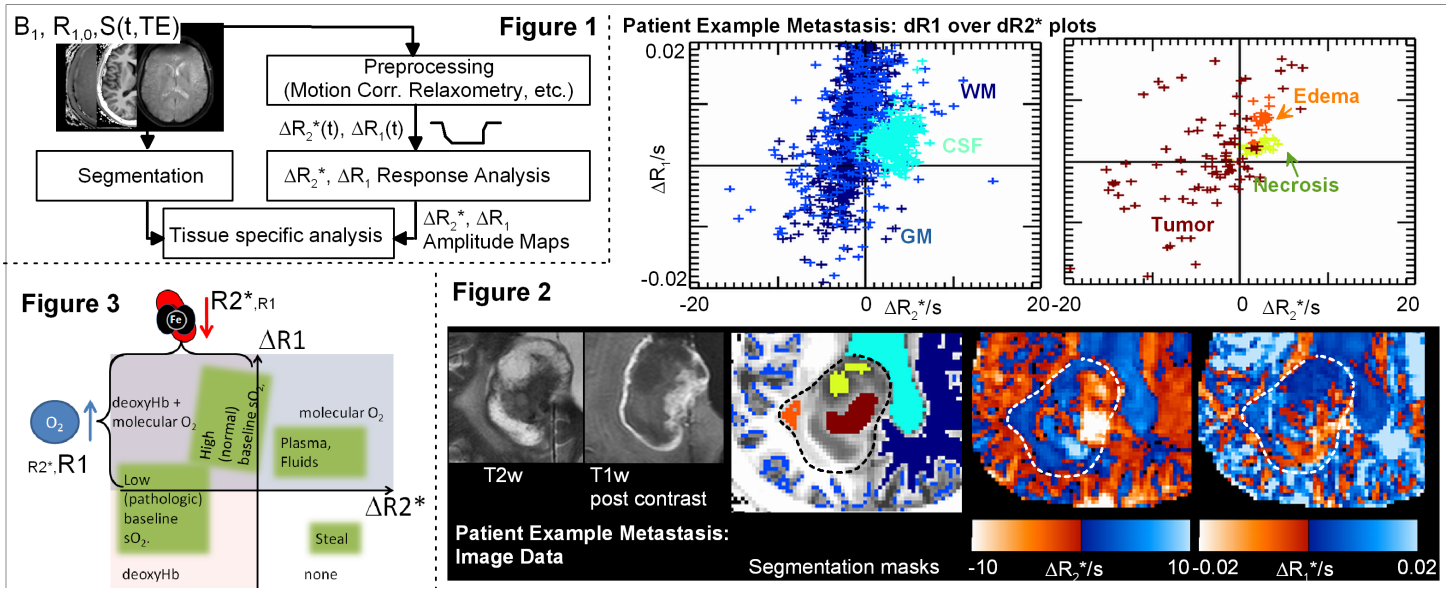


**Fig 1: Processing Workflow. Fig.2 Upper row: $\Delta R_1$ over $\Delta R_2$* plots of the tissue-specific voxel-wise response amplitudes. The different colors represent different segmented areas as depicted in the segmentation mask below. Lower row: Imaging results, segmentation masks and $\Delta R_1$ over $\Delta R_2$* response maps to the carbogen challenge. Fig. 3: Tissue classification derived from the multi-parametric response findings.**

[1] Neeman M, et al, MRM 45, 2001, [2] Rijpkema M, et al, Int. J. Rad. Onc. Biol. Phys. 53, 2002, [3] O'Connor JPB et al, Int. J. Rad. Onc. Biol. Phys. 75, 2009, [4] Blockley NP, et al, MRM 60, 2008, [5] Burrell JS, et al, ISMRM 18, 4828, 2010, [6] Zhou H, et al, ISMRM 18, 2793, 2010, [7] Müller A, et al, JMRI 32, 2010, [8] Remmele S, et al, ISMRM 18, 5121,2010 [9] Jensen ME, et al, Internet J. Rad. 2, 2001, [10] Remmele S, et al, JMRI 31, 2010